clathrin-coated endocytic vesicles requires GTP hydrolysis, whereas the budding of endoplasmic reticulum vesicles and COP-coated Golgi vesicles does not and occurs even in the presence of GTPγS (*26, 27*). In our cell-free reconstituted assay with the silica-coated plasma membranes, only the latter step (or steps) in the formation of free vesicles can be examined, because the firmly attached silica-coating prevents movement so that new invaginations cannot readily form. Hence, in this assay GTP has stimulated the fission of caveolar invaginations to complete the budding process and create free caveolar vesicles. Because GTP does not stimulate budding in the absence of cytosol (*19*), a specific cytosolic factor (or factors), possibly a guanosine triphosphatase (GTPase), may bind to the caveolae to permit fission. Endothelial cell caveolae have been found to contain various GTPases bound to the membrane (*17*). Further definition of the molecular mechanisms mediating budding remains a challenge for the future.

REFERENCES AND NOTES

1. R. Montesano, J. Roth, A. Robert, L. Orci, *Nature* **296**, 651 (1982); D. Trans, J.-L. Carpentier, F. Sawano, P. Gorden, L. Orci, *Proc. Natl. Acad. Sci. U.S.A.* **84**, 7957 (1987); R. G. Parton, *J. Histochem. Cytochem.* **42**, 155 (1994).
2. C. Huet, J. F. Ash, S. J. Singer, *Cell* **21**, 429 (1980); G. Raposo *et al.*, *Eur. J. Cell Biol.* **50**, 340 (1989); R. I. Goldberg, R. M. Smith, L. Jarett, *J. Cell Physiol.* **133**, 203 (1987); G. E. Palade and R. R. Bruns, *J. Cell Biol.* **37**, 633 (1968); L. Ghitescu, A. Fixman, M. Simionescu, N. Simionescu, *ibid.* **102**, 1304 (1986).
3. A. J. Milici, N. E. Watrous, H. Stukenbrok, G. E. Palade, *J. Cell Biol.* **105**, 2603 (1987); L. Ghitescu and M. Bendayan, *ibid.* **117**, 745 (1992).
4. J. E. Schnitzer, P. Oh, E. Pinney, A. Allard, *ibid.* **127**, 1217 (1994).
5. R. G. Parton, B. Joggerst, K. Simons, *ibid.*, p. 1199.
6. G. L. King and S. M. Johnson, *Science* **227**, 1583 (1985).
7. J. E. Schnitzer, *Trends Cardiovasc. Med.* **3**, 1024 (1993).
8. ——— and P. Oh, *J. Biol. Chem.* **269**, 6072 (1994); *Am. J. Physiol.* **263**, H1872 (1992).
9. J. E. Schnitzer, A. Sung, R. Horvat, J. Bravo, *J. Biol. Chem.* **264**, 24544 (1992); J. E. Schnitzer and J. Bravo, *ibid.* **268**, 7562 (1993).
10. E. J. Smart, D. C. Foster, Y.-S. Ying, B. A. Karmen, R. G. W. Anderson, *J. Cell Biol.* **124**, 307 (1994).
11. N. J. Severs, *J. Cell Sci.* **90**, 341 (1988); B. Van Deurs, P. K. Holm, K. Sandvig, S. H. Hansen, *Trends Cell Biol.* **3**, 249 (1993).
12. M. Bundgaard, J. Frokjaer-Jensen, C. Crone, *Proc. Natl. Acad. Sci. U.S.A.* **76**, 6439 (1979); J. Frokjaer-Jensen, *J. Ultrastruct. Res.* **73**, 9 (1980); M. Bundgaard, *Fed. Proc.* **42**, 2425 (1983); J. Frokjaer-Jensen, R. C. Wagner, S. B. Andrews, P. Hagman, T. S. Reese, *Cell Tissue Res.* **254**, 17 (1988); J. J. Frokjaer-Jensen, *J. Electron Microsc. Tech.* **19**, 291 (1991).
13. K. G. Rothberg, Y. Ying, J. F. Kolhouse, B. A. Kamen, R. G. W. Anderson, *J. Cell Biol.* **110**, 637 (1990); R. G. W. Anderson, B. A. Kamen, K. G. Rothberg, S. W. Lacey, *Science* **255**, 410 (1992).
14. J. E. Schnitzer, D. P. McIntosh, A. M. Dvorak, J. Liu, P. Oh, *Science* **269**, 1435 (1995); J. E. Schnitzer, P. Oh, B. S. Jacobson, A. M. Dvorak, *Proc. Natl. Acad. Sci. U.S.A.* **92**, 1759 (1995).
15. Cytosol was isolated from rat lungs perfused as described (*8, 14*). The lungs were flushed free of blood, perfused with cold protease inhibitors, and homogenized in ice-cold cytosolic buffer (2× v/w) (25 mM KCl, 2.5 mM Mg acetate, 5 mM EGTA, 150 mM K acetate, and 25 mM Hepes titrated to a final pH of 7.4 with KOH). The homogenate was centrifuged at 100,000*g* for 1 hour at 4°C, and the supernatant was collected. This cytosol was filtered with a prepacked DG-10 column (Bio-Rad), and samples were stored frozen at −80°C. Unless indicated otherwise, the filtered cytosol (final concentration, 5 mg/ml) was supplemented just before experimentation with 2 mM ATP and an ATP-regeneration system of creatine phosphokinase (16.7 U/ml) and 16.7 mM phosphocreatine.
16. A cell-free assay for caveolar fission was reconstituted with the silica-coated luminal endothelial cell plasma membranes purified from rat lungs as described (*14*). The silica-coated membranes were mixed gently for 0 to 120 min at 37°C with cytosol (*15*) containing 1 mM GTP (unless indicated otherwise) before the addition of ice-cold 60% sucrose in 20 mM KCl to achieve a final 30% sucrose concentration. The mixture was layered onto a cushion of 40% sucrose in a SW55 centrifuge tube, and then 20% sucrose was added to the tube before topping with 20 mM KCl. After centrifugation for 2 hours (30,000 rpm in a SW55 rotor) at 4°C, the pellet containing the silica-coated membranes was processed for immunoblot analysis and densitometric quantification of the signal as described (*14, 17*). For isolation of released caveolae, the membranes were treated as above with 1 mM GTP for 60 min, except that centrifugation was performed with a continuous sucrose gradient as described (*15*).
17. J. E. Schnitzer, J. Liu, P. Oh, *J. Biol. Chem.* **270**, 14399 (1995).
18. J. E. Schnitzer, P. Oh, E. Pinney, J. Allard, *Am. J. Physiol.* **268**, H48 (1995); D. Predescu, R. Horvat, S. Predescu, G. E. Palade, *Proc. Natl. Acad. Sci. U.S.A.* **91**, 3014 (1994).
19. J. E. Schnitzer, P. Oh, D. P. McIntosh, unpublished data.
20. A. M. Fra, E. Williamson, K. Simons, R. G. Parton *J. Biol. Chem.* **269**, 30745 (1994); A. Gorodinsky and D. A. Harris *J. Cell Biol.* **129**, 619 (1995).
21. S. Mayor, K. G. Rothberg, F. R. Maxfield, *Science* **264**, 1948 (1994).
22. The purified silica-coated plasma membranes did not contain detectable ε-COP or other intracellular organelle markers (*14, 19*).
23. T. V. Kurzchalia *et al.*, *J. Cell Biol.* **118**, 1003 (1992); P. Dupree, R. G. Parton, G. Raposo, T. V. Kurchalia, K. Simons, *EMBO J.* **12**, 1597 (1993); D. Brown and J. K. Rose, *Cell* **68**, 533 (1992).
24. For permeabilization, the cells were cooled to 4°C for 10 min and washed once with ice-cold buffer A [20 mM Hepes, 110 mM NaCl, 2 mM $CaCl_2$, 5.4 mM KCl, 0.9 mM Na_2HPO_4, 10 mM $MgCl_2$, 11 mM glucose (pH 7.4)]. Reduced SLO dissolved in buffer A at 0.6 U/ml was bound at 4°C for 10 min before washing twice in ice-cold buffer A and incubation in buffer A at 37°C for 15 min to induce pore formation in the plasma membranes.
25. J. E. Schnitzer, A. Siflinger-Birnboim, P. J. Del Vecchio, A. B. Malik, *Biochem. Biophys. Res. Commun.* **199**, 11 (1994).
26. S. A. Tooze, U. Weiss, W. B. Huttner, *Nature* **347**, 207 (1990); M. F. Rexach and R. W. Schekman, *J. Cell Biol.* **114**, 219 (1991); L. L. Carter, T. E. Redelmeier, L. A. Woolenweber, S. L. Schmid, *ibid.* **120**, 37 (1993).
27. V. Maholtra, T. Serafini, L. Orci, J. C. Shepherd, J. E. Rothman, *Cell* **58**, 329 (1989); R. Schwaninger, H. Plutner, G. M. Bokoch, W. E. Balch, *J. Cell Biol.* **119**, 1077 (1992).
28. E. J. Smart, Y.-S. Ying, C. Mineo, R. W. G. Anderson, *Proc. Natl. Acad. Sci. U.S.A.* **92**, 10104 (1995).
29. J. E. Schnitzer and P. Oh, *Am. J. Physiol.* **270**, 416 (1996).

30. We are indebted to R. Jahn, R. A. Skidgel, M. Krieger, and J. P. Luzio for supplying antibodies to VAMP, ACE, ε-COP, and 5′NT, respectively. Supported by the Beth Israel Hospital Foundation, a Grant-in-Aid from the American Heart Association, and NIH grants HL43278 and HL52766 (J.E.S.). Work for this study was carried out during the tenure of an Established Investigatorship Award from the American Heart Association and Genentech (J.E.S.).

24 July 1996; accepted 20 August 1996

Association of Spindle Assembly Checkpoint Component XMAD2 with Unattached Kinetochores

Rey-Huei Chen, Jennifer C. Waters, E. D. Salmon, Andrew W. Murray*

The spindle assembly checkpoint delays anaphase until all chromosomes are attached to a mitotic spindle. The *mad* (mitotic arrest–deficient) and *bub* (budding uninhibited by benzimidazole) mutants of budding yeast lack this checkpoint and fail to arrest the cell cycle when microtubules are depolymerized. A frog homolog of *MAD2* (*XMAD2*) was isolated and found to play an essential role in the spindle assembly checkpoint in frog egg extracts. XMAD2 protein associated with unattached kinetochores in prometaphase and in nocodazole-treated cells and disappeared from kinetochores at metaphase in untreated cells, suggesting that XMAD2 plays a role in the activation of the checkpoint by unattached kinetochores. This study furthers understanding of the mechanism of cell cycle checkpoints in metazoa and provides a marker for studying the role of the spindle assembly checkpoint in the genetic instability of tumors.

The cell division cycle is a highly ordered and tightly regulated process. Its transitions are monitored by checkpoints that delay the cell cycle until critical events are completed (*1–3*). Accurate chromosome segregation requires that chromosomes attach to and become aligned on the mitotic spindle before activation of the cyclin proteolysis machinery induces sister chromatid separation, cyclin B degradation, and loss of histone H1 kinase activity of $p34^{cdc2}$. Inhibition of spindle assembly with microtubule

Fig. 1. Amino acid sequence comparison between XMAD2 and its human, yeast, and *C. elegans* homologs. Residues that are conserved in all species are shown in bold. Sequences used to design degenerate PCR oligonucleotides are indicated by a horizontal line above the sequence. Abbreviations for the amino acid residues are as follows: A, Ala; C, Cys; D, Asp; E, Glu; F, Phe; G, Gly; H, His; I, Ile; K, Lys; L, Leu; M, Met; N, Asn; P, Pro; Q, Gln; R, Arg; S, Ser; T, Thr; V, Val; W, Trp; and Y, Tyr.

```
                                                                                                  60
Xenopus          MAGQLTRE.G ITLKGSAEIV SEFFFCGINS ILYQRGIYPS ETFTRIQKYG LTLLVSTDPA
Human            MALQLSREQG ITLRGSAEIV AEFFSFGINS ILYQRGIYPS ETFTRVQKYG LTLLVTTDLE
C. elegans                                                                       GTRKK
Budding yeast          MSQS ISLKGSTRTV TEFFEYSINS ILYQRGVYPA EDFVTVKKYD LTLLKTHDDE

                                                                                                 120
Xenopus          LKEYLNKVTD QLKDWLYKCQ VQKLVVVITS IDSNEILERW QFDIECDKTV KDG..IVREK
Human            LIKYLNNVVE QLKDWLYKCS VQKLVVVISN IESGEVLERW QFDIECDKTA KDD.SAPREK
C. elegans       LQAFMDPLLQ QVEYWLAKRQ LKRLVMVISE VKTKEVVERW QFDIHTENLA EEGENAHRVK
Budding yeast    LKDYIRKILL QVHRWLLGGK CNQLVLCIVD KDEGEVVERW SFNVQHISGN SNGQDDVVD.

                                                                                                 180
Xenopus          SQKVIQEEIR SVIRQITATV TFLPLL..ET ACAFDLLIYT DKDLEVPEKW EESGPQFVSN
Human            SQKAIQDEIR SVIRQITATV TFLPLL..EV SCSFDLLIYT DKDLVVPEKW EESGPQFITN
C. elegans       EEKKIRQEIS DVIRQITASV SFLPL
Budding yeast    .LNTTQSQIR ALIRQITSSV TFLPELTKEG GYTFTVLAYT DADAKVPLEW ADSNSKEIPD

Xenopus          SEEVRLRSFT TTIHKVNSMV AYK.KIDTF
Human            SEEVRLRSFT TTIHKVNSMV AYKIPVND
Budding yeast    GEVVQFKTFS TNDHKVGAQV SYKY
```

depolymerizing drugs, such as nocodazole and benomyl, activates the spindle assembly checkpoint and prevents the onset of anaphase. Components of this checkpoint have been isolated in the budding yeast *Saccharomyces cerevisiae*. Mutations in the *MAD* (*4*, *5*) or *BUB* (*6*, *7*) genes result in premature exit from mitosis and cell death when spindle assembly is inhibited. A spindle assembly checkpoint also has been described in frog egg extracts (*8*). The checkpoint is activated and anaphase is inhibited when mitotic extracts are incubated with nocodazole and sperm nuclei at a density of greater than 9000 nuclei per microliter, a nucleocytoplasmic ratio comparable with that of somatic cells. Under these conditions, mitogen-activated protein kinase activity is essential for activation and maintenance of the checkpoint, but the other components involved in sensing spindle assembly and chromosome alignment are unknown (*8*).

The identification of human (*9*) and *Caenorhabditis elegans* (GenBank accession number T01775) *MAD2* homologs allowed us to isolate a cDNA encoding a *Xenopus* homolog by degenerate polymerase chain reaction (PCR). This gene (*XMAD2*; GenBank accession number U66167) contains an open reading frame of 203 amino acids that encode a protein with a predicted molecular size of 23 kD, with 41 and 81% identity with the yeast and human sequences, respectively (Fig. 1). Despite its similarity with yeast Mad2, XMAD2 did not rescue the benomyl sensitivity of a *mad2* mutant when expressed by a strong galactose-inducible promoter (*10*). Affinity-purified antibodies to XMAD2 (anti-XMAD2) specifically recognized a 25-kD protein in frog egg extracts, frog fibroblast cell line XTC, and human HeLa cells (Fig. 2A).

We used anti-XMAD2 to determine the role of XMAD2. Cytostatic factor (CSF)–arrested frog egg extracts are stably arrested at

R.-H. Chen and A. W. Murray, Department of Physiology, University of California, San Francisco, San Francisco, CA 94143, USA.
J. C. Waters and E. D. Salmon, Department of Biology, University of North Carolina, Chapel Hill, NC 27599, USA.
* To whom correspondence should be addressed.

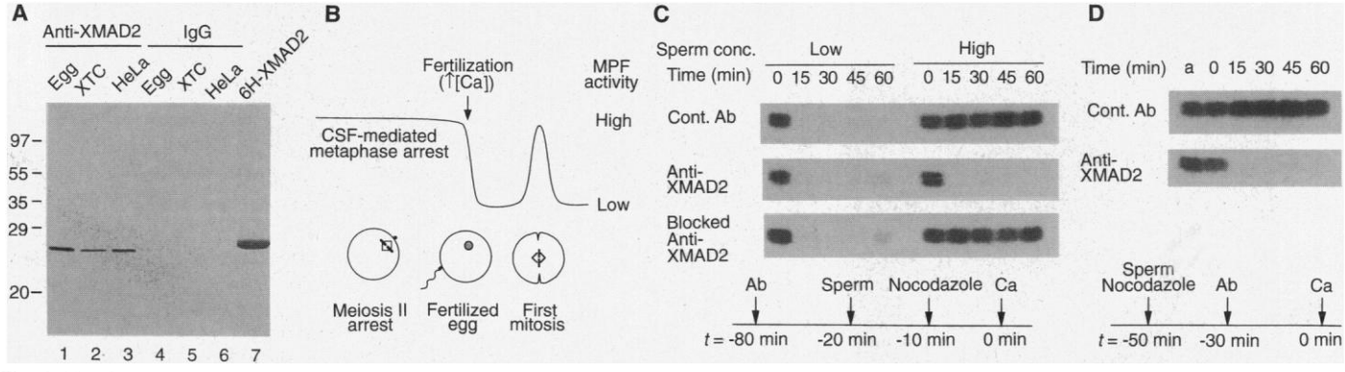

Fig. 2. XMAD2 is essential for the spindle assembly checkpoint in frog egg extracts. (**A**) Specificity of affinity-purified anti-XMAD2. Immunoblot with affinity-purified anti-XMAD2 (*23*) (lanes 1 to 3) or with control IgG (*23*) (lanes 4 to 6) of proteins from CSF-arrested frog egg extracts (lanes 1 and 4), *Xenopus* tissue culture cell lysate (lanes 2 and 5), and HeLa cell lysate (lanes 3 and 6) (*24*). Lane 7, purified recombinant XMAD2 (6H-XMAD2) (4 μg) (*25*). Positions of molecular size standards (in kilodaltons) are indicated on the left. (**B**) Schematic representation of early stages of the *Xenopus* life cycle. MPF, maturation promoting factor. (**C**) Inhibition of the spindle assembly checkpoint in CSF-arrested extracts by anti-XMAD2. Autoradiograms of histone H1 kinase assays (*22*) from CSF-arrested extracts at the indicated times after calcium was added to overcome the action of CSF. Before high or low concentrations of sperm nuclei and nocodazole were added to activate the spindle assembly checkpoint, the extracts were incubated with (top to bottom) control antibodies (Con. Ab), affinity-purified anti-XMAD2, and anti-XMAD2 that had been incubated with 6H-XMAD2 (blocked). (**D**) Disruption of checkpoint maintenance by anti-XMAD2. The spindle assembly checkpoint was first activated by adding nocodazole and a high concentration of sperm nuclei to CSF-arrested extracts (lane a). Control antibodies or anti-XMAD2 were then added for 30 min before calcium was added (lane 0). Samples were taken every 15 min and H1 kinase activity measured. The experimental procedures are also indicated schematically below (C) and (D) (*t*, time) and are described in (*26*). Results shown are representative of at least three independent experiments.

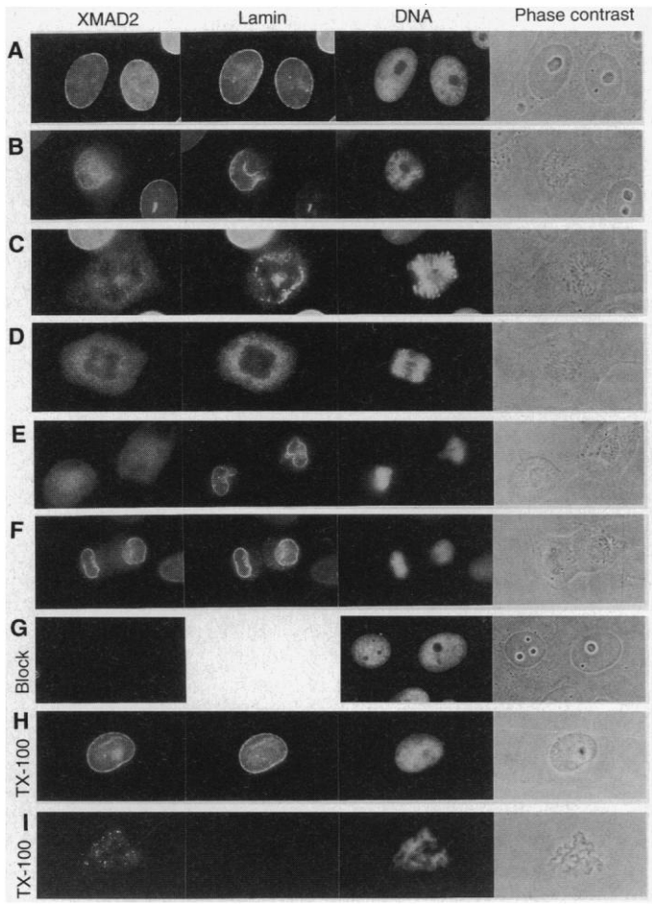

Fig. 3. Localization of XMAD2 to the nuclear envelope and the nucleus at interphase. (**A** to **F**) Asynchronous XTC cells were fixed and stained with anti-XMAD2 or a monoclonal antibody to lamin B as indicated. Cells presented from top to bottom panels are at interphase and at various stages of mitosis and cytokinesis. (**G**) Cells were stained with anti-XMAD2 that had been incubated with 6H-XMAD2. (**H** and **I**) Cells were extracted with Triton X-100 (TX-100) before fixation. Anti-XMAD2 purified from two different rabbits gave essentially the same staining pattern. Phase-contrast photographs and corresponding nuclei stained with the DNA dye Hoechst 33258 are also shown. Cells were prepared for immunofluorescent staining as described (*27*).

metaphase, with high histone H1 kinase activity associated with a CDC2-cyclin B complex, and can enter interphase in response to added calcium (*11*, *12*) (Fig. 2B). Activation of the spindle assembly checkpoint makes these extracts insensitive to calcium addition and prevents inactivation of H1 kinase activity (*8*). We tested whether the addition of anti-XMAD2 to extracts affects the spindle assembly checkpoint. Extracts containing anti-XMAD2 maintained active H1 kinase before calcium addition, suggesting that this antibody has no effect on CSF-mediated mitotic-phase arrest. At low sperm density, the addition of calcium to extracts treated with either control antibodies or anti-XMAD2 led to rapid inactivation of H1 kinase, consistent with the previous demonstration (*8*) that the spindle assembly checkpoint is not active at low nuclear density (Fig. 2C). At high sperm densities, extracts treated with control antibodies maintained high H1 kinase activity for at least 60 min after calcium addition, showing that the spindle assembly checkpoint had been activated. In contrast, extracts treated with anti-XMAD2 did not maintain high H1 kinase activity (Fig. 2C) and the sperm chromosomes decondensed and formed interphase nuclei (*13*), indicating that the antibody inhibited the spindle assembly checkpoint. This inhibitory activity appeared to be specific for XMAD2, because anti-XMAD2 that had been incubated with recombinant 6H-XMAD2 pro-

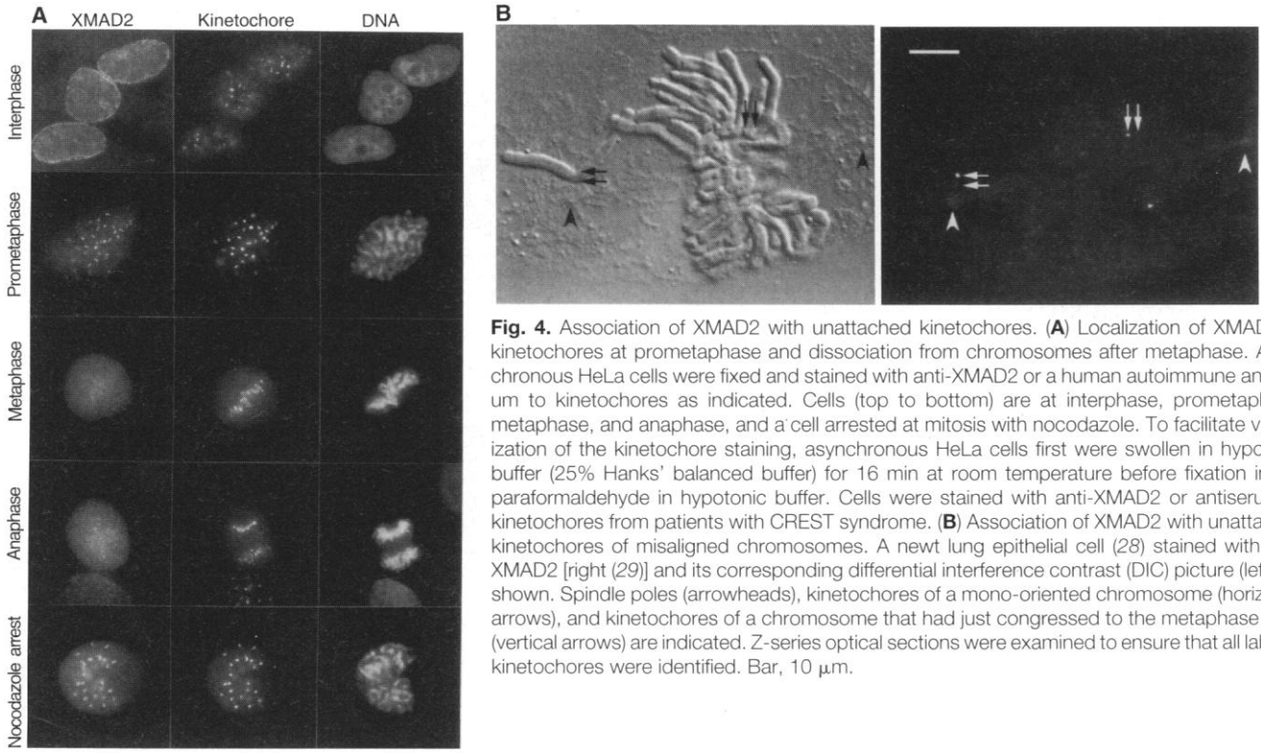

Fig. 4. Association of XMAD2 with unattached kinetochores. (**A**) Localization of XMAD2 to kinetochores at prometaphase and dissociation from chromosomes after metaphase. Asynchronous HeLa cells were fixed and stained with anti-XMAD2 or a human autoimmune antiserum to kinetochores as indicated. Cells (top to bottom) are at interphase, prometaphase, metaphase, and anaphase, and a cell arrested at mitosis with nocodazole. To facilitate visualization of the kinetochore staining, asynchronous HeLa cells first were swollen in hypotonic buffer (25% Hanks' balanced buffer) for 16 min at room temperature before fixation in 3% paraformaldehyde in hypotonic buffer. Cells were stained with anti-XMAD2 or antiserum to kinetochores from patients with CREST syndrome. (**B**) Association of XMAD2 with unattached kinetochores of misaligned chromosomes. A newt lung epithelial cell (*28*) stained with anti-XMAD2 [right (*29*)] and its corresponding differential interference contrast (DIC) picture (left) are shown. Spindle poles (arrowheads), kinetochores of a mono-oriented chromosome (horizontal arrows), and kinetochores of a chromosome that had just congressed to the metaphase plate (vertical arrows) are indicated. Z-series optical sections were examined to ensure that all labeled kinetochores were identified. Bar, 10 μm.

tein had no effect on H1 kinase activity. When the checkpoint was first activated by incubating CSF-arrested extracts with a high concentration of sperm nuclei and nocodazole (Fig. 2D, lane a) followed by addition of anti-XMAD2, calcium addition still inactivated H1 kinase, indicating that XMAD2 is required for maintenance of the checkpoint (Fig. 2D).

We examined localization of XMAD2 during the cell cycle (Fig. 3). In interphase cells of an asynchronous XTC culture, anti-XMAD2 predominantly stained the nuclear envelope, with minor staining in the nucleus (Fig. 3A). The staining was blocked if the antibodies were first incubated with recombinant XMAD2 (Fig. 3G), indicating that the staining was specific to XMAD2. The nuclear envelope staining pattern was very similar to that of the nuclear lamins (Fig. 3A). In prophase cells, in which the nuclear envelope is dissolving, XMAD2 showed diffuse cytoplasmic staining before the lamins were completely disassembled (Fig. 3, B and C). After cytokinesis, anti-XMAD2 did not localize onto the nuclear envelope until the assembly of nuclear lamin had begun (Fig. 3, E and F). Like the lamins, association of XMAD2 with the nuclear envelope in interphase cells was resistant to detergent extraction (Fig. 3H). These results suggest that XMAD2 may interact either directly or indirectly with components of the nuclear lamins during interphase.

During mitosis, essentially all of the lamin protein becomes soluble and can be removed from cells by detergent treatment before fixation (Fig. 3I). Although detergent extracted the bulk of XMAD2 from mitotic cells, some of the protein remained and stained as paired dots associated with condensed chromosomes (Fig. 3I). Because this pattern was reminiscent of staining seen with antibodies to kinetochores, we compared the staining patterns of XMAD2 and kinetochores. No antibody was available that recognized frog kinetochores throughout the cell cycle, so we used HeLa cells in which kinetochores could be stained with an autoimmune serum from patients with CREST syndrome (calcinosis, Raynaud's phenomenon, esophageal dysmotility, sclerodactyly, telangiectasia) (*14*). In interphase HeLa cells, anti-XMAD2 stained the nuclear envelope and the nucleus (Fig. 4A). In prometaphase HeLa cells, anti-XMAD2 stained paired dots in addition to a diffuse cytoplasmic staining (Fig. 4A). All of the dots colocalized with the CREST serum staining (Fig. 4A), showing that vertebrate MAD2 localizes at the kinetochores of sister chromatids in prometaphase cells. In metaphase and anaphase cells, anti-XMAD2 was not localized to kinetochores (Fig. 4A), whereas kinetochore staining with the CREST serum was clearly visible. Thus, the absence of XMAD2 staining at kinetochores at these stages was not the result of a general inability of antibodies to bind to the kinetochores of highly condensed chromosomes.

The loss of kinetochore-associated XMAD2 staining from metaphase cells is consistent with the possibility that XMAD2 binds only to kinetochores on chromosomes that are not attached to microtubules, although we cannot exclude the possibility that microtubule binding masks the epitope on XMAD2 that our antibodies recognize. The observation that anti-XMAD2 stained kinetochores in nocodazole-arrested mitotic cells supports this notion (Fig. 4A). Furthermore, in newt lung epithelial cells, in which the large spindle makes it possible to follow the movement of individual chromosomes, the unattached kinetochores of mono-oriented chromosomes were labeled consistently with anti-XMAD2, whereas the attached kinetochores were labeled very weakly or not at all (Fig. 4B). In cells that were fixed while a chromosome was congressing to the metaphase plate, the newly attached and leading kinetochore was labeled but the previously attached sister kinetochore was not. Kinetochores that had been at the metaphase plate for longer periods were not labeled (Fig. 4B). These results suggest that the loss of XMAD2 from kinetochores is related to microtubule attachment rather than how long the cells have been in mitosis. The staining pattern of anti-XMAD2 in XTC and newt lung cells was essentially identical to that in HeLa cells (*10*), indicating that the regulated association of XMAD2 at kinetochores is evolutionarily conserved. The large pool of free XMAD2 may exist to ensure that kinetochores that are not bound to microtubules rapidly bind XMAD2 and activate the spindle assembly checkpoint.

The spindle assembly checkpoint inhibits anaphase in cells that lack spindles (*4*, *6*) or have chromosomes that are incorrectly aligned on the spindle. In budding yeast, a single aberrantly segregating minichromosome can activate the spindle-assembly checkpoint (*15*); in animal cells, kinetochores that are not attached to microtubules or are not under tension can inhibit the onset of anaphase (*16*, *17*). The observation that XMAD2, an essential component of the spindle assembly checkpoint, appears at unattached kinetochores during prometaphase and disappears after attachment by microtubules suggests a potential role for XMAD2 as part of the machinery by which unattached kinetochores activate the checkpoint. The kinetochore-association pattern of XMAD2 is very similar to that of a labile phosphoepitope recognized by monoclonal antibody 3F3/2 (*18*, *19*). This epitope is present on kinetochores that are not attached to or are incorrectly aligned on the spindle but disappears as chromosomes orient correctly (*18–20*). XMAD2 is unlikely to be the protein detected by 3F3/2, because we cannot detect posttranslational modification of XMAD2 (*10*). It remains to be determined whether a protein associated with XMAD2 carries the 3F3/2 epitope seen at unattached kinetochores.

Our results demonstrate that the spindle assembly checkpoint is evolutionarily conserved and has an important role in the cell division cycle. XMAD2 provides a useful tool for analyzing the mechanism of the spindle assembly checkpoint in vertebrates as well as a molecular marker that can be used to investigate whether lesions in this checkpoint contribute to the genetic instability of tumor cells.

REFERENCES AND NOTES

1. L. H. Hartwell and T. A. Weinert, *Science* **246**, 629 (1989).
2. A. W. Murray, *Curr. Opin. Cell Biol.* **6**, 872 (1994).
3. ———, *Curr. Opin. Genet.* **5**, 5 (1995).
4. R. Li and A. W. Murray, *Cell* **66**, 519 (1991).
5. K. G. Hardwick and A. W. Murray, *J. Cell Biol.* **131**, 709 (1995).
6. M. A. Hoyt, L. Totis, B. T. Roberts, *Cell* **66**, 507 (1991).
7. B. T. Roberts, K. A. Farr, M. A. Hoyt, *Mol. Cell. Biol.* **14**, 8282 (1992).
8. J. Minshull, H. Sun, N. K. Tonks, A. W. Murray, *Cell* **79**, 475 (1995).
9. Y. Li and R. Benezra, *Science* **274**, 246 (1996).
10. R.-H. Chen and A. W. Murray, unpublished results.
11. M. Lohka and J. Maller, *J. Cell Biol.* **101**, 518 (1985).
12. K. E. Sawin and T. J. Mitchison, *ibid.* **112**, 925 (1991).
13. R.-H. Chen and A. W. Murray, data not shown.
14. S. Brenner, D. Pepper, M. W. Berns, E. Tan, B. R. Brinkley, *J. Cell Biol.* **91**, 95 (1981).
15. W. A. E. Wells and A. W. Murray, *ibid.* **133**, 75 (1996).
16. X. Li and B. Nicklas, *Nature* **373**, 630 (1995).
17. C. L. Rieder, R. W. Cole, A. Khodjakov, G. Sluder, *J. Cell Biol.* **130**, 941 (1995).
18. M. S. Cyert, T. Scherson, M. W. Kirschner, *Dev. Biol.* **129**, 209 (1988).
19. G. J. Gorbsky and W. A. Ricketts, *J. Cell Biol.* **122**, 1311 (1993).
20. R. B. Nicklas, S. C. Ward, G. J. Gorbsky, *ibid.* **130**, 929 (1995).
21. R.-H. Chen, C. Sarnecki, J. Blenis, *Mol. Cell. Biol.* **12**, 915 (1992).
22. A. W. Murray, *Methods Cell Biol.* **36**, 581 (1991).
23. Affinity purification of anti-XMAD2 was done as described (*21*). The control antibody, immunoglobulin G (IgG), was purified from preimmune serum over a protein A column made from Affi-Prep Protein A (Bio-Rad 156-0006) as described [E. Harlow and D. Lane, *Antibodies* (Cold Spring Harbor Laboratory Press, Cold Spring Harbor, NY, 1988)]. Purified antibodies were dialyzed and concentrated in antibody dilution buffer [10 mM sodium phosphate (pH 7.4), 100 mM potassium chloride, 1 mM magnesium chloride, 50% glycerol (v/v)].
24. XTC cells were maintained at 28°C in 70% L-15 medium (Gibco) supplemented with fetal bovine serum (FBS) (10%), penicillin (100 units/ml), and streptomycin (100 μg/ml) (Pen/Strep). HeLa cells were grown in Dulbecco's modified Eagle's medium [with glucose (4.5 g/liter), Gibco] containing 10% FBS and Pen/Strep. Cell lysates were prepared by resuspending the cell pellets or diluting the egg extracts with 10 volumes of lysis buffer [10 mM potassium phosphate (pH 7.5); 1 mM EDTA; 1 mM EGTA; 10 mM magnesium chloride; 50 mM β-glycerophosphate; 1 mM sodium orthovanadate; 1% Triton X-100; 1 mM phenylmethylsulfonyl fluoride; and leupeptin, pepstatin, and chymostatin (each at 10 μg/

ml)] on ice for 10 min followed by centrifugation at 10,000*g* for 5 min at 4°C. Proteins (20 μg) from the supernatants were loaded in each lane and an immunoblot was prepared with ECL (Amersham).
25. To make recombinant XMAD2, we tagged the full-length XMAD2 coding sequence with six histidines at the NH_2-terminus and expressed it in *Escherichia coli* with Qiaexpress vector pQE10 (Qiagen). The protein was purified according to the manufacturer's instructions. The purified proteins were dialyzed against a buffer containing 50 mM Hepes (pH 7.4), 50 mM potassium chloride, and 50% glycerol.
26. Freshly prepared CSF-arrested extracts (20 μl) were first incubated for 1 hour on ice with 1 μl (0.7 μg) of various antibodies. To block anti-XMAD2, we incubated the antibodies with 6H-XMAD2 (antibody:protein = 3:2 by weight or 1:2 in molar ratio) on ice for 1 hour. The extracts were then incubated with a low or high concentration (3000 or 10,000 nuclei per microliter, respectively) of demembranated sperm nuclei prepared as described (*22*) for 10 min at room temperature and for another 10 min at room temperature with nocodazole (10 μg/ml). The nocodazole stock was made in dimethyl sulfoxide at 10 mg/ml and was diluted 1:50 (200 μg/ml) in CSF-arrested extract before it was added to the reaction mixture. CSF-arrested extracts were incubated with a high concentration of sperm nuclei and nocodazole for 20 min and then with control antibodies or anti-XMAD2 at room temperature for 30 min. Calcium chloride (0.4 to 0.6 mM) was added to induce exit from mitosis and 1-μl samples were taken every 15 min and left on dry ice until all of the samples were ready for histone H1 kinase activity measurement as described (*22*).
27. XTC cells were fixed in 3% paraformaldehyde, and immunofluorescent staining was done as described (*21*), except that all buffers were made in 70% phosphate-buffered saline (PBS). For detergent extraction, cells were first extracted with 70% PBS with 0.5% Triton X-100 (PBST) for 5 min followed by fixation with paraformaldehyde. The images were viewed with a Nikon Microphot-FXA microscope and photographed with Kodak Tri-X pan 400 film.
28. C. L. Rieder and R. Hard, *Int. Rev. Cytol.* **122**, 153 (1990).
29. Cells were first simultaneously extracted and fixed with 0.5% Triton X-100, 2% formaldehyde in PHEM [60 mM Pipes, 25 mM Hepes (pH 7), 10 mM EGTA, 2 mM magnesium chloride] for 5 min and then fixed further in 4% formaldehyde in PHEM for 15 min. Immunofluorescent staining was then performed as described (*19*), except that the buffer PBS plus 0.05% Tween 20 was used. Z-series optical sections (0.5 μm thick) were captured with a multimode digital fluorescence microscope system. A Nikon Microphot-FXA microscope equipped with a ×60, numerical aperture 1.4 objective was used.
30. We thank A. Desai and T. Mitchison for the CREST serum and for their expertise and encouragement; J. Minshull for the *Xenopus* ovary cDNA library; R. Benezra, Y. Li, and T. Gustafson for sharing unpublished results; and T. Mitchison, D. Morgan, A. Desai, and members of A.W.M.'s laboratory for their helpful comments on the manuscript. Supported by grants from NIH, the Packard Foundation, the Markey Foundation, and the March of Dimes to A.W.M. R.-H.C. is a Helen Hay Whitney postdoctoral fellow.

14 June 1996; accepted 12 August 1996

Identification of a Human Mitotic Checkpoint Gene: *hsMAD2*

Yong Li and Robert Benezra*

In *Saccharomyces cerevisiae*, *MAD2* is required for mitotic arrest if the spindle assembly is perturbed. The human homolog of *MAD2* was isolated and shown to be a necessary component of the mitotic checkpoint in HeLa cells by antibody electroporation experiments. Human, or *Homo sapiens*, MAD2 (hsMAD2) was localized at the kinetochore after chromosome condensation but was no longer observed at the kinetochore in metaphase, suggesting that MAD2 might monitor the completeness of the spindle-kinetochore attachment. Finally, T47D, a human breast tumor cell line that is sensitive to taxol and nocodazole, had reduced MAD2 expression and failed to arrest in mitosis after nocodazole treatment. Thus, defects in the mitotic checkpoint may contribute to the sensitivity of certain tumors to mitotic spindle inhibitors.

During mitosis, the onset of anaphase is demarcated by the separation of sister chromatids and the destruction of cyclin B, which are irreversible events that commit a cell to complete the division cycle (*1*). Mitotic checkpoint control mechanisms (*2*) test the cell's preparedness to undergo division and block cell cycle progression before the irreversible events associated with anaphase if the mitotic spindle apparatus is not appropriately assembled (*3*, *4*) or if the kinetochore is not properly attached to the spindle (*5*). In budding yeast, six nonessential genes have been identified that are required for the execution of the mitotic checkpoint: *MAD1*, *MAD2*, and *MAD3* (*3*), and *BUB1*, *BUB2*, and *BUB3* (*4*). These genes were identified in screens for mutants that are hypersensitive to drugs that inhibit mitotic spindle assembly by depolymerizing microtubules. A similar mitotic checkpoint pathway also exists in higher eukaryotes (*5*), but its molecular components have not yet been identified.

We isolated a human cDNA clone (*6*) in a screen for high copy number suppressors of thiabendazole (a mitotic spindle assembly inhibitor) sensitivity in yeast cells lacking CBF1, a component of the kinetochore (*7*). Sequence determination of the cDNA revealed an open reading frame (ORF) of 205 amino acids (GenBank accession number U65410) that is similar to that of the product of the mitotic checkpoint gene *MAD2* from the budding yeast, *S. cerevisiae*. The two proteins are 40% identical and 60% similar over the entire ORF (Fig. 1A). We therefore refer to the human MAD2 homolog as hsMAD2. The hsMAD2 protein is also similar to a MAD2 homolog from *Xenopus laevis*, termed XMAD2 (*8*) (Fig. 1A). The protein encoded by hsMAD2 cDNA has a predicted molecular size of 23.5 kD with two putative amphipathic α helices at residues 64 to 74 and 124 to 134. The fact that both *hsMAD2* and yeast *MAD2*, termed *scMAD2*, can partially suppress the thiabendazole sensitivity of *cbf1* null yeast cells (*9*) suggests that without *CBF1*, the mitotic checkpoint is not fully activated.

To further characterize hsMAD2, we generated polyclonal antibodies and affinity-purified them (*10*). Immunoglobulin G (IgG) fractions from preimmune serum and serum raised against hsMAD2 that was first passed over an hsMAD2 affinity column (referred to as anti-hsMAD2Δ) were also isolated (*10*). Protein immunoblot analysis (*11*) revealed that the affinity-purified anti-hsMAD2 specifically recognized a single protein of approximately 24 kD in HeLa cell extracts that was not detected with either preimmune IgG or anti-hsMAD2Δ (Fig. 1B). Extracts from HeLa cells that had been transiently transfected with an expression vector that encodes hsMAD2 showed increased intensity of the 24-kD band, indicating that this protein is probably encoded by the hsMAD2 cDNA (Fig. 1B). Thus, the affinity-purified antibody to hsMAD2 was highly specific for the protein expressed in human cells.

To determine if *hsMAD2* functions as a mitotic checkpoint gene, we introduced affinity-purified anti-hsMAD2 into HeLa cells by electroporation and determined the status of the mitotic checkpoint (*12*). When cells were electroporated with either the preimmune IgG, the anti-hsMAD2Δ, or buffer alone, many of them became rounded after nocodazole treatment, which is indicative of cells arrested in mitosis (Fig. 2). In contrast, cells electroporated with anti-hsMAD2 showed fewer rounded cells after nocodazole treatment (~80 to 90% of the cells that survived the electroporation took up IgG, as assayed by immunofluorescence). We measured the percentage of IgG^+ cells in mitosis (the mitotic index, MI) after nocodazole treatment of the electroporated cells. The average MI of the IgG^+ cells electroporated with either the preimmune IgG or the anti-hsMAD2Δ was about 30% (471 of 1588

Cell Biology and Genetics Program, Memorial Sloan-Kettering Cancer Center, 1275 York Avenue, New York, NY 10021, USA.

*To whom correspondence should be addressed.